1   **Middle Miocene climate of southwestern Anatolia from multiple botanical proxies**

3   Johannes M. Bouchal[1,2], Tuncay H. Güner[3], Thomas Denk[1]

4   [1]Department of Palaeobiology, Swedish Museum of Natural History, 10405 Stockholm,

5   Sweden

6   [2]Department of Palaeontology, University of Vienna, 1090 Vienna, Austria

7   [3]Faculty of Forestry, Department of Forest Botany, Istanbul University, 34473 Bahceköy,

8   Istanbul, Turkey

10   **Correspondence to**: Johannes M. Bouchal (johannes.bouchal@nrm.se) and Thomas Denk

11   (thomas.denk@nrm.se)

16   **Abstract**

17   The middle Miocene climate transition (MMCT) was a phase of global cooling possibly

18   linked to decreasing levels of atmospheric CO_2. The MMCT coincided with the European

19   Mammal Faunal Zone MN6. From this time, important biogeographic links between Anatolia

20   and eastern Africa include the hominid *Kenyapithecus*. Vertebrate fossils suggested mixed

21   open and forested landscapes under (sub)tropical seasonal climates for Anatolia. Here, we

22   infer the palaeoclimate during the MMCT and the succeeding cooling phase for a middle

23   Miocene (14.8–13.2 Ma) of an intramontane basin in southwestern Anatolia using three

24   palaeobotanical proxies: (i) Köppen signatures based on the nearest-living-relative principle.

25   (ii) Leaf physiognomy analysed with the Climate Leaf Analysis Multivariate Program

26   (CLAMP). (iii) Genus-level biogeographic affinities of fossil floras with modern regions.

27   The three proxies reject tropical climates for the MMCT of southwestern Anatolia and instead

28   infer warm temperate *C* climates. Köppen signatures reject summer-dry *Cs* climates but

29   cannot discriminate between fully humid *Cf* and winter-dry *Cw*; CLAMP reconstructs *Cf*

30   climate based on the low X3.wet/X3.dry ratio. Additionally, we assess whether the

31   palaeobotanical record does resolve transitions from the warm Miocene Climatic Optimum

32   (MCO, 16.8–14.7 Ma) into the MMCT (14.7–13.9 Ma), and a more pronounced cooling at

33   13.9–13.8 Ma, as reconstructed from benthic stable isotope data. For southwestern Anatolia,

34   we find that arboreal taxa predominate in MCO floras (MN5), whereas in MMCT floras

35   (MN6) abundances of arboreal and non-arboreal elements strongly fluctuate indicating higher

36   structural complexity of the vegetation. Our data show a distinct pollen zone between MN6

37   and MN7+8 dominated by herbaceous taxa. The boundary MN6 and MN7+8, roughly

38   corresponding to a first abrupt cooling at 13.9–13.8 Ma, possibly might be associated with

39   this herb-rich pollen zone.

40

41   **Keywords**: Miocene; plant fossil; climate proxy; Köppen signatures; CLAMP; biogeography

1 Introduction

42

43 The middle Miocene (15.97–11.63 Ma, ICS-chart 2017/02, Cohen, 2013) is characterized by

44 a warm phase lasting until ca. 15 Ma that was followed by a gradual cooling and the

45 restoration of a major Antarctic ice sheet and first northern hemispheric glaciations (Holbourn

46 et al., 2014). It has been suggested that the final closure of the Mediterranean gateway

47 connecting the Mediterranean with the Indian Ocean and the resulting changes in ocean

48 circulation might have been one of the reasons for the final expansion of the East Antarctic

49 ice sheet around 14.8 Ma (Flower & Kennett, 1993). During the middle Miocene climate

50 transition (MMCT) at 14.7 to 13.8 Ma a drop of sea surface temperatures of 6–7°C occurred

51 (Shevenell et al., 2004). At the same time, different proxies to reconstruct atmospheric CO_2

52 levels for the Miocene Climatic Optimum (MCO), MMCT, and the succeeding more

53 pronounced cooling, do not concur (Beerling & Royer, 2011). Specifically, stable isotope data

54 from phytoplankton infer stable CO_2 levels for the Neogene, with minor fluctuations (MCO,

55 227–327 ppm, MMCT, 265–300 ppm; Beerling & Royer, 2011, table S1), while stomata

56 densities from fossil leaves suggest a pronounced drop of CO_2 after the MCO (Beerling &

57 Royer, 2011, table S1).

58 The European Mammal Faunal Zone MN6 (14.8–13.8 Ma; Neubauer et al., 2015) coincides

59 with the MMCT. From this period world-famous vertebrate faunas are known from western

60 Anatolia (e.g. Andrews & Tobien, 1977; Mayda et al., 2015) including the hominoids

61 *Griphopithecus alpani* in Çandır and Paşalar, and *Kenyapithecus kizili* in Paşalar (Stringer &

62 Andrews, 2011). Geraads et al. (2003) investigated the depositional environment and large

63 mammal fauna of Çandır close to Ankara and inferred open landscapes for this locality.

64 Bernor et al. (1979, p. 86) analysed community structure of Turkish and European middle

65 Miocene faunas and suggested that "*faunas adapted to woodland conditions were present …*

66 *at localities such as Paşalar and Yeni Eskihisar* [MN7-8]" while the "*Çandır fauna has a*

67 *community structure more suggestive of closed woodland conditions*". This interpretation is

68   the exact opposite of that by Geraads et al. (2003). Recent investigations using carnivore guild

69   structure suggest a "*mixed environment between tropical forest and open savannah*

70   *landscape*s" for Çandır and Paşalar (Mayda et al., 2015). Strömberg et al. (2007) investigated

71   phytoliths (plant silica bodies) from early to late Miocene deposits of Turkey and suggested

72   that open, grass-dominated habitats had become common in Turkey and adjacent areas by the

73   early Miocene (c. 20 Ma). In contrast, Kayseri-Özer (2017) using 'integrated plant record'

74   (IPR) analysis (Kovar-Eder et al., 2008) suggested that various forest types covered most of

75   western and Central Anatolia during the middle Miocene (*broad-leaved evergreen* and *mixed*

76   *mesophytic forests* and ecotones between these forests).

77   Here we use a large data set from recently published macrofossils and pollen, spores and cysts

78   from a well-dated middle Miocene basin in western Anatolia to infer palaeoclimate and

79   palaeoenvironments using three palaeobotanical proxies: climate affinity of modern analogues

80   ('nearest living relatives'; taxon-based approach), leaf physiognomy (a-taxonomic), and

81   biogeographic affiliation of plant communities (also taxon-based). The following research

82   questions are addressed: How do the three approaches resolve local climate conditions of

83   Anatolia during a phase of global cooling, ca. 15–13 million years ago? Do different proxies

84   agree on climate inference? Where do modern climates occur that correspond to middle

85   Miocene climates of western Anatolia? Can the palaeobotanical record resolve transitions

86   between MCO, MMCT, and the succeeding more pronounced cooling during the middle

87   Miocene?

88

89   **2 Material and methods**

90   **2.1 Geological setting**

91   The Yatağan Basin is a southeast trending graben (50 km long, 15 km wide) in the province

92   of Muğla, southwestern Turkey (Fig. 1). The Neogene basin fill is up to 600 m thick and

93   divided into the Eskihisar Formation (early to middle Miocene), the Yatağan Formation (late

94   Miocene to early Pliocene), and the Milet Formation (middle to late Pliocene; Alçiçek, 2010).

95   The Eskihisar Formation comprises the Turgut Member (reddened alluvial-fan deposits

96   followed by fluviatile deposits and lignites) and the Sekköy Member (fossiliferous limnic

97   marls and limestones); all economically exploited lignite seams of the Yatağan Basin are

98   confined to the transition zone of these two members (Atalay, 1980; Becker-Platen, 1970).

99   For the present study, we investigated the palaeobotanical content (pollen and plant

100   macrofossils) of the upper Turgut and the Sekköy members exposed at the lignite mines of

101   Eskihisar, Salihpaşalar, and Tınaz (Fig. 1.2). The age of the investigated sediments is well

102   constrained by mammal fossils (Eskihisar lignite gallery locality, MN6, *Gomphotherium*

103   *angustidens* Cuvier 1817, *Percrocuta miocenica* Pavlov et Thenius 1965, Bouchal et al.,

104   2017; Yeni Eskihisar vertebrate locality, MN 7/8, The NOW Community, 2018), and by

105   radiometric dates from the upper Sekköy Member (13.2 Ma ± 0.35, Becker-Platen et al.,

106   1977). Hence, the investigated pollen zones (PZ) 1, 2, 2/3, and the Yeni Eskihisar pollen

107   assemblage represent the Neogene mammal zones MN6 and MN7+8, 14.8–13.2 Ma;

108   Neubauer et al., 2015). The layers from which most of the leaf fossils originate correspond to

109   PZ 2. A ~20 m section comprised of limestone and clayey limestone between PZ 2/3 and the

110   Yeni Eskihisar assemblage is barren of palynological content (Fig. 2).

111

112   **2.2 Plant material**

113   The investigated plant material comprises roughly 1800 macrofossils (mainly leaf fossils)

114   collected between 2010 and 2017. Macrofossils represent 77 taxa, of which five belong to

115   gymnosperms and 72 to angiosperms. Pollen, spores and cysts from five pollen zones (Fig. 2)

116   represent 182 taxa, of which one is a fungus, 9 are algae, 17 moss or fern allies spores, 15

117   gymnosperms, and 140 angiosperms (Supplementary Material S1; for taxonomic descriptions

118   of the plant taxa see Yavuz-Işık et al., 2011; Bouchal et al., 2016, 2017; Bouchal, in press;

119   Güner et al., 2017).

120

2.3 Köppen signatures

Fossil taxa that are resolved to genus or sectional level were represented by extant members

of the genera and sections as modern analogues. First, for accepted taxa (IPNI,

http://www.ipni.org/index.html; most recent regional floras and monographs) their

distribution ranges were determined. Then, 26 Köppen-Geiger climate types (see

Supplementary Material S2 for detailed explanation of Köppen-Geiger climate types, and

Kottek et al., 2006; Peel et al., 2007, Rubel et al., 2017; Global_1986-2010_KG_5m.kmz)

were mapped on modern distribution ranges using Google Earth to establish 'Köppen

signatures' (Denk et al. 2013) for each modern analogue. Representation of different climate

types was first scored for each species within a genus as present (1)/absent (0). To summarize

preferences for climate types of all modern analogues, we used an implicit weighting scheme

to discriminate between modern analogues that are highly decisive (climatically constrained)

vs. those that can be found in many climate zones. The sum of each modern species' Köppen

signature is always one. For example, *Tilia chingiana* is present in two Köppen-Geiger

climate types, *Cfa* and *Cfb,* which count as 0.5 for each type , while *Tilia americana* is present

in ten Köppen-Geiger climate types (*As*, *Aw*, *Cfa*, *Cfb*, *Dfa*, *Dfb*, *Cwa*, *Cwb*, *BSk*, *BWh*), all

counting as 0.1. The Köppen signature of a genus or section, the modern analogue of a fossil

taxon, is the sum of its species' Köppen signatures for each climate type divided by the total

number of scored species for this genus. By this, the percentage representation of each

Köppen-Geiger climate type was determined for a genus/ section. In case of *Tilia*, the

distribution ranges of 26 species resulted in a genus Köppen signature as follows: *Cfa*, 22.1%,

Cfb, 14.7%, *Cwa*, 19.9%, *Cwb*, 9.1%, *Dfb*, 5.7%, for the five most common climate types.

Fig. 3.1 shows all climate types realized in genus *Tilia*; Fig. 3.2 shows that the genus occurs

predominantly in *Cf* and *Cw* Köppen-Geiger climate types and that tropical and desert

145   climates are nearly absent (see Supplementary Material S3 for genus-level scoring of Köppen-

146   Geiger climate types for all plant taxa encountered in the Yatağan basin fossil assemblages).

147   For taxa that are resolved to family-level only, mainly pollen taxa of herbaceous and a few

148   woody angiosperm groups, the distributions of extant members of the family were combined

149   into a general family distribution range and the corresponding Köppen-Geiger climate types

150   determined.

151   Genus-level Köppen-Geiger signals were used to account for possible niche evolution within

152   lineages/ species groups of a genus. For example, modern species of *Quercus* section *Ilex* are

153   typical members of sclerophyllous, evergreen Mediterranean forest and shrubland vegetation

154   thriving under a *Cs* (summer-dry warm temperate) climate in western Eurasia and along the

155   western parts of the southern foothills of the Himalayas, but also occur in humid, mesophytic

156   forests from Afghanistan to East Asia (*Cf* and *Cw* climates). To account for this climate niche

157   variability, all species of sect. *Ilex* were scored for the general Köppen signature of sect. *Ilex*.

158   Hence, the entire section was used as modern analogue, the nearest living relative (NLR), for

159   several fossil species of *Quercus* sect. *Ilex*.

160

161   **2.4 CLAMP**

162   We inferred quantitative palaeoclimate parameters for the three Yatağan Basin floras using

163   the Climate Leaf Analysis Multivariate Program (CLAMP) (Yang et al., 2011). CLAMP

164   makes use of the relationship between leaf physiognomy and climate and, hence, is a non-

165   taxonomic approach to palaeoclimate inference (Spicer, 2008). Modern and fossil leaf

166   physiognomic data are positioned in multidimensional physiognomic space using high

167   resolution gridded climate data and canonical correspondance analysis. For details on the

168   methodology see the CLAMP website (http://clamp.ibcas.ac.cn).

169   For the present study, 36 different leaf characters were scored for 61, 63, and 14

170   dicotyledonous leaf morphotypes from three localities, Tınaz, Eskihisar, and Salihpaşalar (see

171   Supplementary Material S4 for scoring of morphotypes), following the CLAMP protocols

172   (http://clamp.ibcas.ac.cn). At genus level, the floras of the Yatağan Basin show highest

173   similarity with Eurasian extant woody angiosperms (Table 1), thus the PhysgAsia1

174   Calibration files dataset of CLAMP was used to position the fossil data.

175

176   *2.5 Genus level biogeographic affinities*

177   For all fossil taxa determined to genus level, the present distribution was tabulated indicating

178   presence/absence of a genus in western Eurasia, East Asia, eastern North America, western

179   North America, and Africa (Table 1).

180

181   **3 Results**

182   **3.1 Climate inference from Köppen signatures** (Fig. 5, Supplementary Materials S5, S6)

183   For the fossil plant assemblages warm temperate to temperate *C* and *D* climates accounted for

184   almost 80% of the realized Köppen-Geiger climate types of all taxa in a fossil plant

185   assemblage (using genus-level NLR). The sum of *Cf*, *Df*, *Cw* and *Dw* climates amounted to

186   60–70% in all assemblages (highest scores in macrofossil assemblages).

187   Overall, the best represented Köppen-Geiger climate types when using genus-level NLR were

188   *Cfa* (warm temperate, fully humid, hot summer), followed by *Cfb* (warm temperate, fully

189   humid, warm summer), *Cwa* (warm temperate, winter-dry, hot summer), and *Cwb* (warm

190   temperate, winter-dry, warm summer). Summer-dry *Cs* climates were represented by 9–13%

191   and arid (generally dry) *B* climates by 6–11% (Supplementary Materials S2, S5). Tropical

192   (equatorial) climates (*A*) are represented by 9–11% in older assemblages, and 7–8% in the

193   two youngest assemblages (PZ 2/3 and Yeni Eskihisar). Of 1555 modern species used to

194   inform the Köppen signatures of the NLRs for the fossil taxa, 119 show (marginal???) range

195   extensions into *Af* climate, 168 into *Am* (heavy monsoon), 85 into *As*, and 295 into *Aw*

196   (Supplementary Material S3). Taxa extending in tropical climates are mainly species of

197   *Celtis*, *Smilax*, and *Viburnum*, *Quercus* sections *Quercus* and *Lobatae*, Juglandaceae

198   subfamily Engelhardioideae, Oleaceae, and Sapotaceae. Exclusion of Köppen-Geiger climate

199   signals extracted from cosmopolitan and/or gymnospermous taxa did not change the general

200   trends (Supplementary Material S6).

201

202   **3.2 CLAMP**

203   Sixty-three morphotypes were scored for Eskihisar (Fig. 6; see Supplementary Material S4 for

204   score sheets and other reconstructed climate parameters). Inferred values for mean annual

205   temperature (MAT) were (11.2–) 12.6 (–14) °C, for coldest month mean temperature

206   (CMMT) (0.3–) 2.3 (–4.4) °C, and for the three wettest months (X3.wet) (410–) 666 (–936)

207   mm and for the three driest months (X3.dry) (148–) 204 (–262) mm. The ratio X3.wet/X3.dry

208   was between 2.9 and 3.6. For Tınaz, the reconstructed MAT was (12.3–) 13.8 (–15.2) °C,

209   CMMT (1.5–) 3.6 (–5.6) °C, X3.wet (420–) 700 (–980) mm, and X3.dry (146–) 205 (–260)

210   mm. The ratio X3.wet/X3.dry was between 2.9 and 3.8. Values for Salihpaşalar are not

211   considered here as they are based on a too small set of morphotypes (see Supplementary

212   Material S4).

213

214   **3.3 Genus level biogeography**

215   The genus-level biogeographic analysis of the four Yatağan Basin floras ranging in age from

216   14.8 to 13.2 Ma (MN6 into MN+/8; Table 1) shows that closest biogeographic relationships

217   are with the modern East Asian flora (54 of 59 taxa shared with East Asia), 48 and 44 genera

218   are shared with the modern western Eurasian and eastern North American floras, respectively.

219   Among modern tropical floras, closest relationships are with South America (21), followed by

220   Africa (16) and northern/ north-eastern Australia (13). Most taxa extending to tropical regions

221   are cosmopolitan (e.g. *Euphorbia*, *Drosera*, *Phragmites*), hence, of little discriminative

222   power. This is also true for higher taxa such as Polygalaceae and Valerianoideae. The fossil

223   species *Smilax miohavanensis* belongs to a subtropical-tropical clade of extant species (Denk

224   et al., 2015) and is the only member of this group in Eurasia; it has its last occurrence in the

225   middle Miocene floras of the Yatağan Basin. Overall, the dominating biogeographic signal is

226   a northern hemispheric one.

227

228   **3.4 Changes in ratios arboreal to non-arboreal pollen**

229   Ratios of arboreal pollen (AP) to non-arboreal pollen (NAP) change considerably among and

230   within pollen zones of the Yatağan Basin assemblages (Table 2, Supplementary Material S7).

231   Pollen zone 1 (main lignite seam) consistently has high percentages of AP (94–70%). In

232   contrast, AP percentage values fluctuate throughout pollen zone 2, with values from 89 to 29.

233   Pollen zone 2-3, only covered in the Tınaz section, records AP percentages of 50 to 19.

234   Above, the MN7+8 assemblage of Yeni Eskihisar shows again a higher proportion of arboreal

235   taxa (67%).

236

237   **4 Discussion**

238   **4.1 Climate inference using Köppen signatures and CLAMP**

239   Using Köppen signatures, we made a semi-quantitative reconstruction of the palaeoclimate of

240   the Yatağan Basin during the middle Miocene. All Köppen signatures used here rely on the

241   nearest-living-relative principle (Denk et al., 2013). Such approaches are prone to error

242   because niche evolution may have occurred in lineages, the morphologically nearest living

243   relatives (NLRs), a species or group of morphologically similar species, of fossil taxa may

244   have different niches, and the shift is difficult to quantify (Ackerly, 2004; Grimm & Potts,

245   2016; Denk et al., 2017). Hence, we opted against applying quantitative NLR methods and

246   determined Köppen signatures for fossil taxa using information from all extant species of a

247   genus used as NLR to avoid bias from undetected niche shifts.

248   It is important to keep climatic niche shift in mind when using NLR based approaches to

249   palaeoclimate inference and interpreting their results (cf. Grimm & Potts, 2016; Denk et al.,

250   2017). In our dataset of 1555 modern species, 295 also occur in tropical *Aw* climates. Most of

251   them belong to clades (monophyletic sections, genera, families) that occur in a wide range of

252   climate types (e.g. Amaranthaceae, *Celtis*, white and red oaks). Others, such as *Engelhardia*

253   are usually interpreted as tropical-subtropical evergreen element (Kvaček, 2007) based on the

254   distribution range of the extant genera of the comprising subfamily, the Engelhardoideae.

255   However, '*Engelhardia*' of the western Eurasian Cenozoic belongs to its own (extinct)

256   section or genus *Palaeocarya* (Kvaček, 2007) with a stratigraphic range from Eocene to

257   Pliocene. Pollen, foliage, and reproductive structures of fossil material clearly belong to

258   subfamily Engelhardioideae but cannot be assigned to just a single modern genus *Engelhardia*

259   (tropical Southeast Asia). Instead the fossil-taxon is a mosaic taxon having characteristics of

260   both American and Asian members of the subfamily. Kvaček (2007) noted that the fossil

261   genus/subgenus flourished in subtropical climates during the Eocene but in distinctly

262   temperate climates with coldest month mean temperatures close to the freezing point in the

263   Neogene, in stark contrast to the surviving four, likely relict genera of the Engelhardioideae.

264   Hence, this extinct lineage of Engelhardioideae is not well represented by a single or the

265   combination of all extant genera and their constituent species. Similarly, representatives of

266   *Smilax havanensis* and allied species are part of a New World clade with most species

267   occurring in tropical climates. However, the single Old World member of the clade, the fossil

268   species *S. miohavanensis*, is known from early to middle Miocene strata of Anatolia and

269   Central Europe (Denk et al., 2015). This fossil species formed part of plant assemblages that

270   rule out tropical climates. In this case, inferring palaeoclimate from extant distribution data

271   only inevitably will produce noise to the climatic signal.

272   Overall, the most common Köppen-Geiger climate types of NLR taxa of the Yatağan floras

273   were warm temperate *C* types, and among *C* types fully humid *Cf* climates were better

274   represented than more seasonal *Cw* and *Cs* types (Fig. 5; Supplementary Material S5). *Cs*

275   types played only a minor role; however, there was no clear preference of *Cf* over *Cw*

276   climates in the representation of Köppen-Geiger climate types. Removing azonal taxa, or taxa

277   commonly associated with higher elevations (conifers) did not affect the general signal.

278   In contrast, CLAMP is not based on NLR and hence not potentially biased by taxonomic

279   error. Its combination with the Köppen signature analysis provides a powerful tool for climate

280   inference and to discern between seasonal *Cw* (winter dry) and *Cs* (summer dry) and fully

281   humid *Cf* climates can be made. Specifically, the ratio of the wettest and the driest month

282   clearly distinguishes strongly seasonal summer rain (monsoon) climates (*Cw*; precipitation

283   wettest month > 10x precipitation driest month, [$P_{wdry/sdry} < P_{wet/wwet}/10$]; Peel et al., 2007)

284   from weakly seasonal, fully humid climates (*Cf*; precipitation wettest month << 10x

285   precipitation driest month). Precipitation values for X3.wet and X3.dry inferred by CLAMP,

286   and the ratio between these ranges being between 2.9 and 3.8 thus largely rules out a *Cw*

287   climate (X3.wet and X3.dry are closely correlated to $P_{dry/wet}$). In conjunction with the Köppen

288   signature results ruling out summer-dry conditions, the CLAMP precipitation and temperature

289   estimates point towards cold subtropical to mild temperate *Cfa* climates at the margin to fully

290   temperate *Cfb* climates.

291

292   **4.2 Comparison to palaeoclimate and palaeoenvironment inferences from other proxies**

293   A further refinement of previous climate and vegetation inferences can be made regarding the

294   distinction between tropical ($T_{min} \equiv CMMT \geq 18$ °C), subtropical (X months with $T \geq 10$° C;

295   ~ MAT of xxx–xxx °C, and CMMT of xxx–xxx °C) and temperate climates. CLAMP

296   consistently resolves MAT < 18 ºC and CMMT < 6 °C for the localities Eskihisar and Tınaz,

297   and this agrees with the results from Köppen signatures and a previous qualitative assessment

298   of palaeoenvironments in the Yatağan Basin (Güner et al., 2017). Both these results, rejecting

299   strongly seasonal *Cw* climates, summer dry *Cs,* and tropical *A* climates (at least for non-

300   coastal areas) for the middle Miocene of western Anatolia, have implications for the

301   reconstruction of palaeoenvironments of famous vertebrate localities in Anatolia that are

302   assigned to MN6. The δ^{13}C composition from fossil tooth enamel at Paşalar, western

303   Anatolia, MN6, indicates that animals were feeding on C_3 vegetation (Quade et al., 1995).

304   The palaeoenvironment for this locality was determined as closer to Indian subtropical

305   forests, with seasonal summer rainfalls (i.e. warm *Cwa* climates), semi-deciduous forest and

306   dense ground vegetation (Stringer & Andrews, 2011; Mayda et al., 2015). Using carnivore

307   guild structures Morlo et al. (2010) inferred open (Serengeti type, *Aw* climate) landscapes for

308   the Central Anatolian MN6 vertebrate locality Çandır. Also, the NOW database

309   (http://www.helsinki.fi/science/now/; The NOW Community, 2018) refers to Çandır as more

310   open ("woodland biome", "open vegetation structure", "grassland with mosaic of forests")

311   and to Paşalar as more forested landscapes ("subtropical", "closed vegetation structure",

312   "semi-deciduous forests"). Bernor et al. (1979) using community structure of vertebrate

313   faunas inferred densely wooded environments for Çandır. In a later study based on a

314   taxonomic revision of carnivores, Mayda et al. (2015) proposed a mixed environment

315   between tropical forests and open savannah landscapes for Çandır. It is important to note that

316   these carnivore guild structure studies used only two modern calibration faunas to estimate

317   palaeoenvironments, one tropical rainforest fauna in Guyana, and one savannah (tropical)

318   fauna in the Serengeti (Morlo et al., 2010). Thus, using this proxy, only two environments can

319   be reconstructed, tropical savannah or rainforest.

320   Our plant-proxy based climate reconstruction unambiguously rejects a tropical climate for the

321   middle Miocene Yatağan Basin and major biogeographic patterns strongly suggest northern

322   hemispheric affinities. Similar environmental conditions as reconstructed in our study have

323   been inferred for most of western Anatolia during the late early and middle Miocene

324   (Kayseri-Özer, 2017). Most proxies currently used to infer climate and vegetation in western

325   Anatolia during the middle Miocene (carnivore guild structures, vertebrate community

326   structure, plant functional types, plant macrofossils, pollen and spores; Mayda et al., 2015,

327   2016; Kayseri-Özer, 2017; Güner et al., 2017; Bouchal et al. 2016, 2017; Bouchal, 2018)

328   clearly infer forested vegetation with varying contributions of open vegetation. In contrast,

329   Strömberg et al. (2007) found that "*all Miocene phytolith assemblages point to relatively open*

330   *vegetation, such as savanna or open woodland dominated by open-habitat grasses, or a*

331   *mixture of grassland and wooded areas*". This result may be strongly biased (see Jokela,

332   2015, p. 44) and increased diversity of grass types in the phytolith record may not actually

333   indicate the presence of widespread open, grass-dominated landscapes.

334

335   **4.3 Modern climate analogues**

336   The inferred climate for the middle Miocene Yatağan Basin plant assemblages is

337   characterized by MAT 11–15 °C, coldest month mean temperature (CMMT) 0–6 °C, MAP

338   ca. 1000–2000 mm, and ratios of X3.wet/X3.dry 2.9–3.8. A non-exhaustive search for climate

339   stations with this combination of climate parameters (Supplementary Material S8) identified a

340   single closest match, Pacific central Honshu of Japan. X3.wet/X3.dry ratios and MAT are

341   similar to the upper limits of the ranges reconstructed for the middle Miocene Yatağan Basin.

342   East Asian *Cf* climates are generally characterized by distinct summer rain maxima. The

343   modern vegetation of Japan is home to many plant taxa that are currently absent from western

344   Eurasia but were abundant in Neogene plant assemblages of western Eurasia (e.g.

345   *Cephalotaxus, Cryptomeria, Torreya, Alangium, Camellia, Castanopsis, Cercidiphyllum,*

346   *Daphniphyllum, Eurya, Fatsia*; Mai, 1995; Miyawaki, 1984; see also Milne, 2004). These

347   taxa require warm and humid equable climates.

348   A further close match is the area from northern Turkey via Georgia to northern Iran, the

349   Euxinian-Hyrcanian region (Supplementary Material S8). Climates at the transition between

350   *Csa* and *Cfa/b* of the region north of Istanbul have up to 1166 mm MAP (Ustaoğlu, 2012) and

351   other climate parameters in this area match the Miocene climate of southwestern Turkey

352   inferred by CLAMP. Towards the humid north-eastern part of Turkey, X3.wet/X3.dry ratios

353   are lower (2.4 for Rize, Hopa and Poti and Kobuleti in adjacent western Georgia). Further to

354   the east, south of the Caspian Sea, Rasht and Kiashahr have *Cfa* and borderline *Csa* to *Cfa*

355   climates with slightly more pronounced seasonality than the reconstructed climate for the

356   Miocene of southwestern Turkey (X3.wet/X3.dry ratios 4.4 and 4.2). In contrast,

357   X3.wet/X3.dry ratios in modern Mediterranean western and southwestern Turkey amount to

358   25 (Izmir) and 21.8 (Muğla, Yatağan Basin). It is noteworthy that modern *Cf* climates of the

359   Euxinian-Hyrcanian region differ markedly from those of the Pacific part of Honshu by their

360   summer minima in rainfall (Supplementary Material S8). This feature indicates a (weak)

361   Mediterranean influence in this region. According to Biltekin et al. (2015) the Anatolian

362   refugium emerged after the retreat of the Paratethys Sea in the Pliocene and increasing

363   monsoon influence (increased summer rainfall???) over the north-eastern Mediterranean

364   region (the latter accounting for the much higher summer precipitation in the Euxinian-

365   Hyrcanian than in the Mediterranean region). The Mediterranean climate type in Europe

366   appeared first during the late Pliocene and early Pleistocene (ca. 3.2–2.3 Ma; Suc, 1984)

367   coinciding with first large-scale north hemispheric glaciation in the North Atlantic (Denk et

368   al., 2011).

369

370   **4.4 Detection of Miocene global climatic changes in the terrestrial fossil record**

371   High-resolution benthic stable isotopic data provide a detailed chronology of (global) climatic

372   changes across the Miocene Climatic Optimum (MCO), the middle Miocene Climatic

373   transition (MMCT), and the subsequent more pronounced cooling (Holbourn et al., 2014).

374   The terrestrial record usually does not provide the same temporal resolution but allows

375   focussing on regional patterns. The transition from MCO to MMCT has previously been

376   documented in high-resolution palynological analyses. For example, Jiménez-Moreno et al.

377   (2005) investigated a core from the Pannonian Basin and observed a decline of megathermic

378   taxa at the transition MCO to MMCT. Also Ivanov & Worobiec (2017) reported a decrease of

379   thermophile taxa for the transition for Bulgaria and Poland. In southwestern Anatolia, Kayseri

380   et al. (2014) investigated three localities in the Muğla-Ören area south of the Yatağan Basin,

381   which are dated by vertebrate fossils as early and late MN5 and thus correspond to the MCO.

382   These authors report a few warmth-loving elements (palms, *Avicennia*) that are missing in the

383   younger strata of the Yatağan Basin. This could be due to the deltaic setting of these floras as

384   opposed to the intramontane setting of the Yatağan Basin floras. In general, the floras of the

385   Muğla-Ören area are very similar to the floras of the Yatağan Basin (Bouchal. et al., 2017).

386   However, a striking difference with the MN6 and MN7+8 assemblages of the Yatağan Basin

387   is the almost entire absence of herbaceous taxa (non-arboreal pollen) in the MN5 assemblages

388   of Ören (Table 2). This may indicate the presence of more closed forest vegetation of the

389   laurisilva type. The assemblages of the Yatağan Basin, show fluctuating arboreal to non-

390   arboreal pollen (AP:NAP) ratios with a peak of NAP in the transition zone MN6 to MN7+8

391   (pollen zone PZ 2–3). This peak could possibly correspond to a sharp cooling detected in the

392   benthic stable isotopic data at 13.9-13.8 Ma (Holbourn et al., 2014). In the European mammal

393   stratigraphy (Neubauer et al., 2015) the boundary MN6 to MN7+8 is at 13.9 Ma. Above PZ

394   2–3, the radiometrically dated Yeni Eskihisar pollen assemblage clearly belongs to MN7+8.

395   Here, woody taxa are again more prominent. Thus, although the correlation of pollen zone 2–

396   3 with the cooling event at 13.9–13.8 Ma is highly speculative, it is clear that the MCO in

397   southwestern Anatolia was characterized by laurisilva vegetation with little contribution of

398   herbaceous taxa. During the MMCT the main woody taxa did not change much, but

399   herbaceous taxa played a much greater role. This indicates higher structural complexity of the

400   vegetation. The presence of early hominids in western Anatolia during this time might be

401   connected to this more complex vegetation. It is unclear at present, whether these changes

402   were accompanied by changes in concentrations of atmospheric CO_2. The compilation of

403   reconstructed CO_2 values across the Cenozoic from hundreds of proxy data (Beerling &

404   Royer, 2011) shows that there is no agreement between different proxies for the MCO and the

405   subsequent middle Miocene climate cooling. Phytoplankton stable isotopic data suggest

406   nearly stable CO_2 concentrations (MCO, 227–327 ppm, MMCT, 265–300 ppm; Beerling &

407   Royer, 2011, table S1). In contrast, stomata densities from fossil leaves suggest a pronounced

408   decline of CO_2 across this interval.

409

410   **Author contribution**

411   JMB and TD designed the study. TD wrote the first draft of the manuscript. TG made the

412   CLAMP analysis, JMB made the Köppen signature analysis. All authors discussed the data

413   and contributed to the final version of the manuscript.

414

415   **Acknowledgements**

416   This work was supported by the Swedish research Council [grant no. 2015-03986 to TD].

417

418   **References**

419   Ackerly, D. D.: Adaptation, niche conservatism, and convergence: comparative studies of leaf
420   evolution in the California chaparral, Am. Nat., 163, 654–671, 2004.
421   Alçiçek, H.: Stratigraphic correlation of the Neogene basins in southwestern Anatolia:
422   Regional palaeogeographical, palaeoclimatic and tectonic implications. Palaeogeogr.
423   Palaeoclimatol. Palaeoecol. 291, 297–318, 2010.
424   Andrews, P. and Tobien, H.: New Miocene locality in Turkey with evidence on the origin of
425   *Ramapithecus* and *Sivapithecus*, Nature, 268, 699–701, 1977.
426   Atalay, Z.: Muğla-Yatağan ve yakın dolayı karasal Neojen'inin stratigrafi araştırması, Bull.
427   Geol. Soc. Turkey, C23, 93–99, 1980.
428   Becker-Platen, J. D.: Lithostratigraphische Untersuchungen im Känozoikum Südwest-
429   Anatoliens (Türkei) (Känozoikum und Braunkohlender der Türkei, 2), Beih. Geol. Jb.,
430   97, 1–244, 1970.
431   Becker-Platen, J. D., Benda, L., and Steffens, F.: Litho- und biostratigraphische Deutung
432   radiometrischer Altersbestimmungen aus dem Jungtertiär der Türkei, Geol. Jb., B25,
433   139–167, 1977.
434   Bernor, R.L., Andrews, P.J., Solounias, N., Van Couvering, J.A.H.: The evolution of
435   "Pontian" mammal faunas: some zoogeographic, palaeoecologic and
436   chronostratigraphic considerations. Annales Géologiques des Pays Helléniques. Tome
437   hors série [special issue] 1979, 1, 81–89, 1979.

Biltekin, D., Popescu, S.-M., Suc, J.-P., Quézel, P., Jiménez-Moreno, G., Yavuz-Işık, N., and
Çağatay, M. N.: Anatolia: A long-time plant refuge area documented by pollen records
over the last 23 million years, Rev. Palaeobot. Palynol., 215, 1–22, 2015.

Bouchal, J. M.: The middle Miocene palynofloras of the Salihpaşalar lignite mine (Yatağan
Basin, southwest Anatolia): environmental characterisation and comparison with coeval
palynofloras from adjacent subbasins, Palaeobiodiversity and Palaeoenvironments, in
Press, 2018.

Bouchal, J. M., Mayda, S., Grímsson, F., Akgün, F., Zetter, R., and Denk, T.: Miocene
palynofloras of the Tınaz lignite mine, Muğla, southwest Anatolia: taxonomy,
palaeoecology and local vegetation change, Rev. Palaeobot. Palynol., 243, 1–36, 2017.

Bouchal, J. M., Zetter, R., Grímsson, F., and Denk, T.: The middle Miocene palynoflora and
palaeoenvironments of Eskihisar (Yatağan Basin, southwestern Anatolia): a combined
LM and SEM investigation, Bot. J. Linn. Soc., 182, 14–79, 2016.

Cohen, K.M., Finney, S.C., Gibbard, P.L., and Fan, J.-X. The ICS International
Chronostratigraphic Chart. *Episodes* 36:199–204, 2013 (updated 2017).
http://www.stratigraphy.org/index.php/ics-chart-timescale

Corbett, S. L. and Manchester, S. R.: Phytogeography and fossil history of *Ailanthus*
(Simaroubaceae), Internatioonal Journal of Plant Sciences, 165, 671–690, 2004.

Denk, T., Grimm, G. W., Grímsson, F., and Zetter, R.: Evidence from "Köppen signatures" of
fossil plant assemblages for effective heat transport of Gulf Stream to subarctic North
Atlantic during Miocene cooling, Biogeosciences, 10, 7927–7942, 2013.

Denk, T., Grímsson, F., Zetter, R., and Símonarson, L. A.: Late Cainozoic Floras of Iceland:
15 Million Years of Vegetation and Climate History in the Northern North Atlantic.,
Springer, Heidelberg, New York, 2011.

Denk, T., Velitzelos, D., Güner, H. T., Bouchal, J. M., Grímsson, F., and Grimm, G. W.:
Taxonomy and palaeoecology of two widespread western Eurasian Neogene
sclerophyllous oak species: *Quercus drymeja* Unger and *Q. mediterranea* Unger, Rev.
Palaeobot. Palynol., 241, 98–128, 2017b.

Denk, T., Velitzelos, D., Güner, H. T., and Ferrufino-Acosta, L.: *Smilax* (Smilacaceae) from
the Miocene of western Eurasia with Caribbean biogeographic affinities, Am. J. Bot.,
102, 423–438, 2015.

Flower, B. P. and Kennett, J. P.: Middle Miocene deepwater paleoceanography in the
southwest Pacific: relations with East Antarctic Ice Sheet development.,
Paleoceanography, 10, 1095-1112, 1995.

Geraads, D., Begun, D., and Güleç, E.: The middle Miocene hominoid site of Çandir, Turkey:
general palaeoecological conclusions from the mammalian fauna, Courier Forschungs-
Institut Senckenberg, 240, 241–250, 2003.

Grimm, G. W. and Potts, A. J.: Fallacies and fantasies: the theoretical underpinnings of the
Coexistence Approach for palaeoclimate reconstruction, Clim. Past, 12, 611–622, 2016.

Güner, H. T., Bouchal, J. M., Köse, N., Göktaş, F., Mayda, S., and Denk, T.: Landscape
heterogeneity in the Yatağan Basin (southwestern Turkey) during the middle Miocene
inferred from plant macrofossils, Palaeontogr. B, 296, 113–171, 2017.

Holbourn, A., Kuhnt, W., Lyle, M., Schneider, L., Romero, and O., Andersen, N.: Middle
Miocene climate cooling linked to intensification of eastern equatorial Pacific
upwelling. Geology, 42, 19–22, 2014.

Inaner, H., Nakoman, E., and Karayigit, A. I.: Coal resource estimation in the Bayir field,
Yatağan-Muğla, SW Turkey, Energy Sources A, 30, 1005–1015, 2008.

Ivanov, D. and Worobiec E.: Middle Miocene (Badenian) vegetation and climate dynamics in
Bulgaria and Poland based on pollen data, Palaeogeogr. Palaeoclimatol. Palaeoecol.,
467, 83–94, 2017.

Jia, L.-B., Manchester, S. R., Su, T., Xing, Y.-W., Chen, W.-Y., Huang, Y.-J., and Zhou, Z.-K.: First occurrence of *Cedrelospermum* (Ulmaceae) in Asia and its biogeographic implications, J. Plant Res., 128, 747–761, 2015.

Jiménez-Moreno, G., Rodríguez-Tovar, F.-J., Pardo-Igúzquiza, E., Fauquette, S., Suc, J.-P., Müller, P.: High-resolution palynological analysis in late early-middle Miocene core from the Pannonian Basin, Hungary: climatic changes, astronomical forcing and eustatic fluctuations in the Central Paratethys. Palaeogeogr. Palaeoclimatol. Palaeoecol., 216, 73–97, 2005.

Jokela, T.: The high, the sharp and the rounded: paleodiet and paleoecology of Late Miocene herbivorous mammals from Greece and Iran. PhD thesis, University of Helsinki. 2015. http://urn.fi/URN:NBN:fi-fe2017112252491.

Kayseri-Özer, M. S.: Cenozoic vegetation and climate change in Anatolia — A study based on the IPR-vegetation analysis, Palaeogeogr. Palaeoclimatol. Palaeoecol., 467, 37–68, 2017.

Kayseri-Özer, M.S., Akgün, F., Mayda, S., Kaya, T.: Palynofloras and vertebrates from Muğla-Ören region (SW Turkey) and palaeoclimate of the Middle Burdigalian–Langhian period in Turkey. Bull. Geosci. 89, 137–162, 2014.

Kottek, M., Grieser, J., Beck, C., Rudolf, B., and Rubel, F.: World map of the Köppen-Geiger climate classification updated., Meteorol. Z., 15, 259-263, 2006.

Kovar-Eder, J., Jechorek, H., Kvaček, Z., and Parashiv, V.: The Integrated Plant Record: An essential tool for reconstructing Neogene zonal vegetation in Europe, Palaios, 23, 97–111, 2008.

Kvaček, Z.: Do extant nearest relatives of thermophile European Cenozoic plant elements reliably reflect climatic signal?, Palaeogeogr. Palaeoclimatol. Palaeoecol., 253, 32-40, 2007.

Kvaček, Z., Velitzelos, D., and Velitzelos, E.: Late Miocene Flora of Vegora, Macedonia, N. Greece, Korali Publications, Athens, 2002.

Magri, D., Di Rita, F., Aranbarri, J., Fletcher, W., González-Sampériz, P.: Quaternary disappearance of tree taxa from Southern Europe: Timing and trends. Quat. Sci. Rev. 163, 23–55, 2017.

Martinetto, E.: The role of central Italy as a centre of refuge for thermophilous plants in the late Cenozoic., Acta Palaeobot., 41, 299–319, 2001.

Mayda, S., Koufos, G. D., Kaya, T., and Gul, A.: New carnivore material from the Middle Miocene of Turkey. Implications on biochronology and palaeoecology, Geobios, 48, 9–23, 2015.

Milne, R. I.: Phylogeny and biogeography of *Rhododendron* subsection *Pontica*, a group with a tertiary relict distribution, Mol. Phylogenet. Evol., 33, 389–401, 2004.

Miyawaki, A.: A vegetation-ecological view of the Japanese archipelago, Bulletin of the Institute of Environmental Science and Technology, 11, 85–101, 1984.

Morlo, M., Gunnell, G. F., and Nagel, D.: Ecomorphological analysis of carnivore guilds in the Eocene through Miocene of Laurasia. In: Carnivoran Evolution: New Views on Phylogeny, Form, and Function, Goswami, A. and Friscia, A. (Eds.), Cambridge University Press, Cambridge, UK, 2010.

Neubauer, T. A., Georgopoulou, E., Kroh, A., Harzhauser, M., Mandic, O., and Esu, D.: Synopsis of European Neogene freshwater gastropod localities: updated stratigraphy and geography, Palaeontogia Electronica, 18.1.3T, 1–7, 2015.

Peel, M. C., Finlayson, B. L., and McMahon, T. A.: Updated world map of the Köppen-Geiger climate classification., Hydrol. Earth System Sci., 11, 1633-1644, 2007.

537 Quade, J. and Cerling, T. E.: Expansion of C4 grasses in the Late Miocene of Northern
538   Pakistan: evidence from stable isotope paleosols., Palaeogeogr. Palaeoclimatol.
539   Palaeoecol., 115, 91–116, 1995.
540 Rubel, F., Brugger, K., Haslinger, K., and Auer, I.: The climate of the European Alps: Shift of
541   very high resolution Köppen-Geiger climate zones 1800–2100. Meteorologische
542   Zeitschrift, 26 (2), 115–125, 2017. DOI:10.1127/metz/2016/0816.
543 Shevenell, A. E., Kennett, J. P., and Lea, D. W.: Middle Miocene Southern Ocean cooling and
544   Antarctic cryosphere expansion., Science, 305, 1766-1770, 2004.
545 Spicer, R. A.: CLAMP. In: Encyclopedia of Paleoclimatology and Ancient Environments
546   Gornitz, V. (Ed.), Springer, Dodrecht, 2008.
547 Stringer, C. and Andrews, P.: The Complete World of Human Evolution, Thames & Hudson,
548   London, 2011.
549 Strömberg, C.A.E., Werdelin, L., Friis, E.M., Saraç, G.: The spread of grass-dominated
550   habitats in Turkey and surrounding areas during the Cenozoic: phytolith evidence.
551   Palaeogeogr., Palaeoclimatol., Palaeoecol. 250, 18–49, 2007.
552 Suc, J.-P.: Origin and evolution of the Mediterranean vegetation and climate in Europe,
553   Nature, 307, 429–432, 1984.
554 The NOW Community.: New and old worlds database of fossil mammals (NOW). Licensed
555   under CC BZ 4.0 Release 2008. Published on the Internet. Last accessed 23-04-2018.
556   http://www.helsinki.fi/science/now/
557 Ustaoğlu, B.: Comparisons of annual meanprecipitation gridded and station data: An example
558   from Istanbul, Turkey, Marmara Coğrafya Dergisi, 26, 71–81, 2012.
559 Wang, Q., Dilcher, D. L., Lott, T. A.: *Podocarpium* A. Braun ex Stizenberger 1851 from the
560   middle Miocene of Eastern China, and its palaeoecology and biogeography. Acta
561   Palaeobot. 47, 237–251, 2007.
562 Yang, J., Spicer, R. A., Spicer, T. E. V., and Li, C.-S.: 'CLAMP Online': a new web-based
563   palaeoclimate tool and its application to the terrestrial Paleogene and Neogene of North
564   America, Palaeobiodiversity and Palaeoenvironments, 91, 163, 2011.
565 Yavuz-Işık, N., Saraç, G., Ünay, E., and de Bruijn, H.: Palynological analysis of Neogene
566   mammal sites of Turkey - Vegetational and climatic implications, Yerbilimeri, 32, 105–
567   120, 2011.
568

569

570 **Supplementary Material.**

571 **S1**: A. Number of fossil-taxa (macrofossils and microfossils) from four middle Miocene

572 localities (including one macrofossil horizon and four pollen zones - PZ) in the Yatağan

573 Basin.

574 B. All fossil-taxa recorded from four Yatağan Basin floras (14.8–13.2 Ma; MN6 into MN7–

575 8).

576 **S2**: Definition of Köppen-Geiger climate types (Kottek et al., 2006, Peel et al., 2007).

577   **S3**: Köppen-Geiger climate type signatures of all genera represented in micro and macrofloras

578   of the Yatağan Basin.

579   **S4**: Coding of leaf physiognomic characters for morphotypes from three macrofloras. Output

580   pdf files from online CLAMP analysis (http://clamp.ibcas.ac.cn).

581   **S5**: Heat maps showing precise representation of different Köppen-Geiger climate types for

582   all fossil assemblages.

583   **S6**: Köppen signature diagrams excluding cosmopolitan and gymnospermous taxa.

584   **S7**: Arboreal to non-arboreal pollen ratios for three sections, of the Yatağan Basin.

585   **S8**: Modern climate stations comparable to the middle Miocene climate of the Yatağan Basin,

586   southwestern Anatolia. Climate data from CLIMATE-DATA.ORG (https://sv.climate-

587   data.org/info/sources/) and Ustaoğlu (2012). Selected Walter-Lieth climate diagrams illustrate

588   qualitative difference between Euxinian-Hyrcanian and Japanese (Honshu) *Cf* climates.

589

590

591

592   **Tables and Figures**
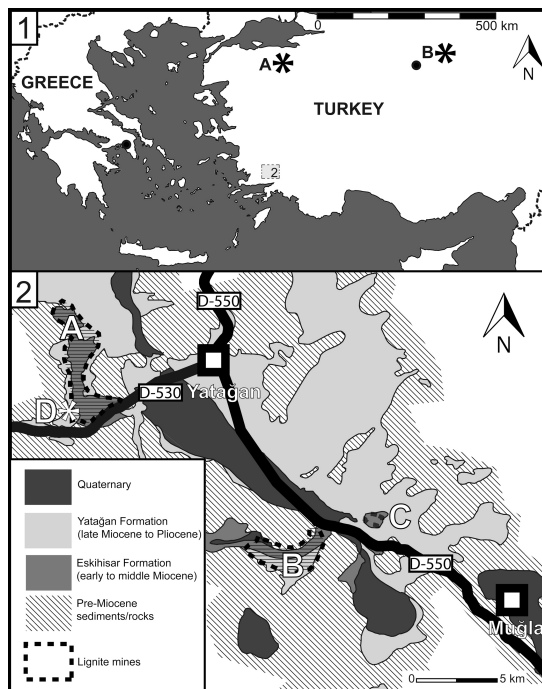
593

594   **Figure 1**. Geographic and regional geologic setting of the Yatağan basin. **1.** Map showing the

595   geographical position of the Yatağan Basin (2) and the MN6 vertebrate fossil localities (*)

596   Paşalar (A) and Çandir (B). **2.** Simplified regional geological map of the Yatağan Basin based

597   on Becker-Platen (1970) and Atalay (1980); lignite mines Eskihisar (A), Tınaz (B),

598   Salihpaşalar (C); vertebrate fossil locality (*) Yeni Eskihisar MN7/8 (D).

599

600
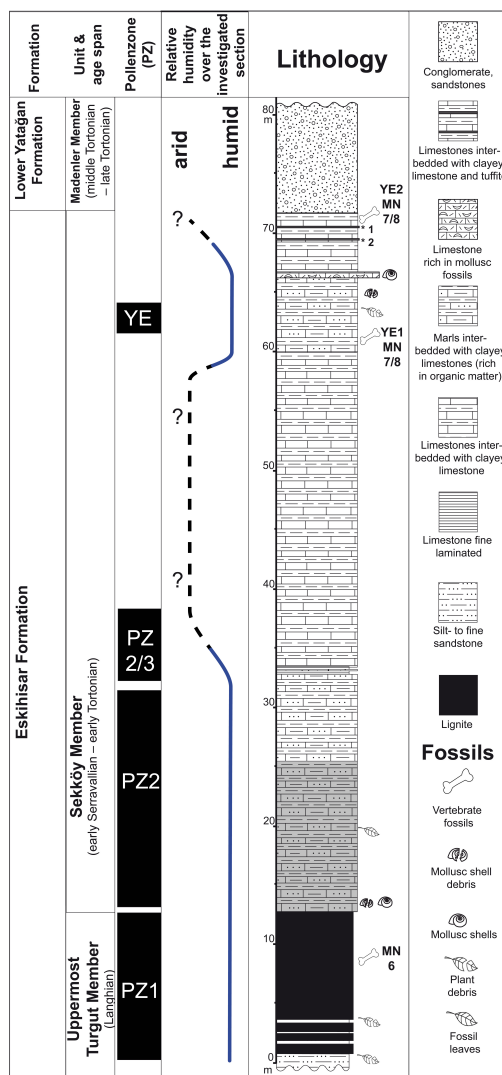
Figure 2. Generalized lithostratigraphic column for the Eskihisar lignite mine and pollen

zones (PZ). The main part of the investigated plant macrofossils originates from ca 10 m thick

deposits overlying the exploited lignite seams (part of the section highlighted in grey

corresponding to PZ 2). Yeni Eskihisar 2 (YE2) and Yeni Eskihisar 1 (YE1) vertebrate fossil

localities (Becker-Platen et al. 1977). Radiometrically dated tuff layers (*), 1* 11.2 ± 0.2 Ma,

2* 13.2 ± 0.35 Ma (Becker-Platen et al. 1977).

607

608
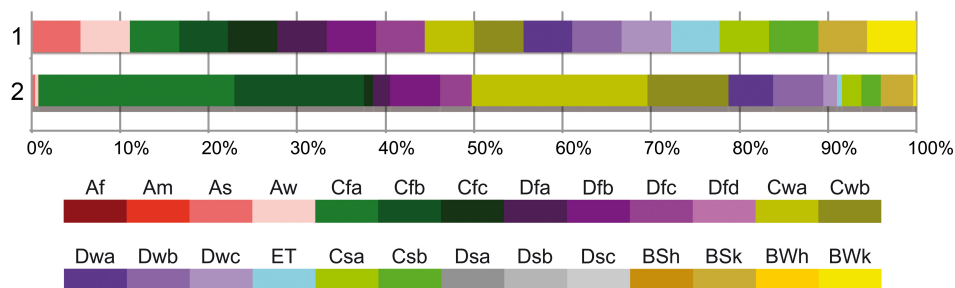
Figure 3. Köppen signal for genus *Tilia* extracted from 26 extant species. **1**. Köppen-Geiger

climates in which *Tilia* is present. **2**. Combined Köppen signature of all 26 extant *Tilia*

species.

612
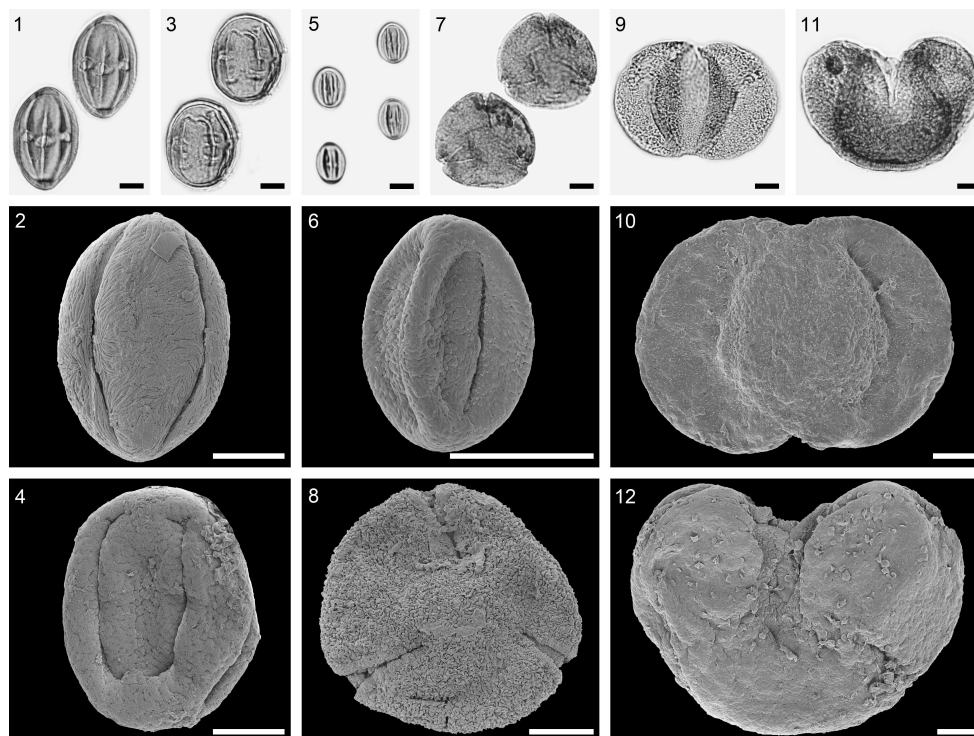
Figure 4. Selected pollen grains LM (1, 3, 5, 7, 9, 11) and SEM (2, 4, 6, 8, 10, 12)

micrographs of the same fossil pollen grain of the Eskihisar (E), Tınaz (T), and Salihpaşalar

(S) sections. **1–2**. *Nitraria* sp., EV (E, S153567). **3–4**. Sapotaceae gen. indet., EV (T,

S143604). **5–6**. *Decodon* sp., EV (S, S153635). **7–8**. *Fagus* sp., PV (T, S143621). **9–10**.

Cathaya sp., (9) PV, (10) PRV (S, S153632). **11–12**. *Cedrus* sp., EV (E, S153590).

EV = equatorial view, PV = polar view, PRV = proximal view. Scale bar = 10μm (1–12).

621
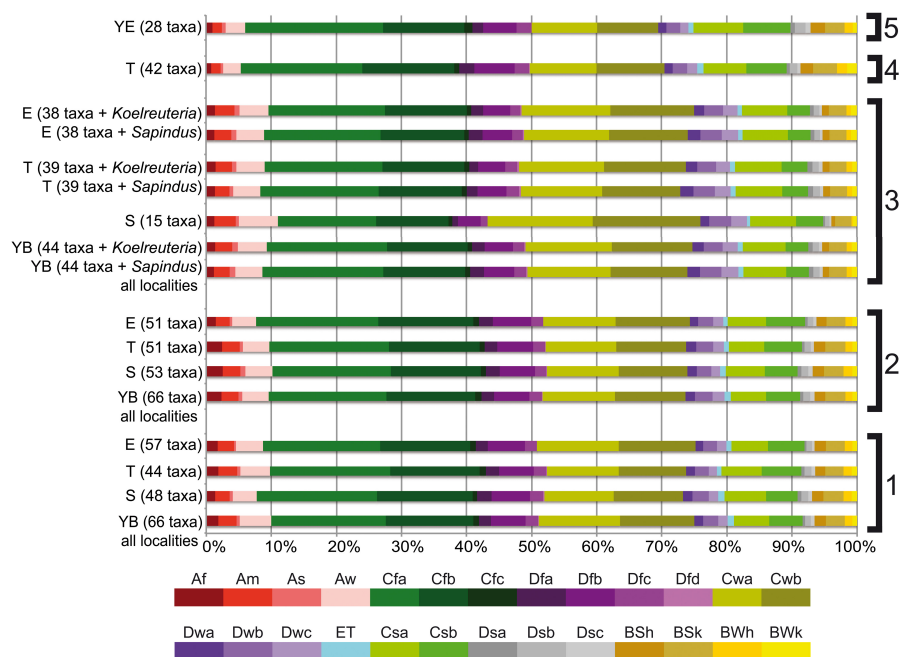
Figure 5. Köppen signals for the Yatağan Basin floras. **1.** Pollen zone (PZ) 1 (MN6; 14.95–

13.9 Ma) of the Eskihisar (E), Tınaz (T), and Salihpaşalar (S) localities and the combined

signal of all present taxa from PZ 1 of the three Yatağan Basin localities (YB). **2.** PZ 2 (MN6)

of E, T, S, YB. **3.** Macrofossil (MF) assemblages (same level as PZ 2) of E, T, S. **4.** PZ 2/3 of

T. (younger than Yeni Eskihisar vertebrate locality). **5.** Yeni Eskihisar vertebrate locality

pollen assemblage (MN7/8, younger than radiometric age 13.2 Ma).

628

629
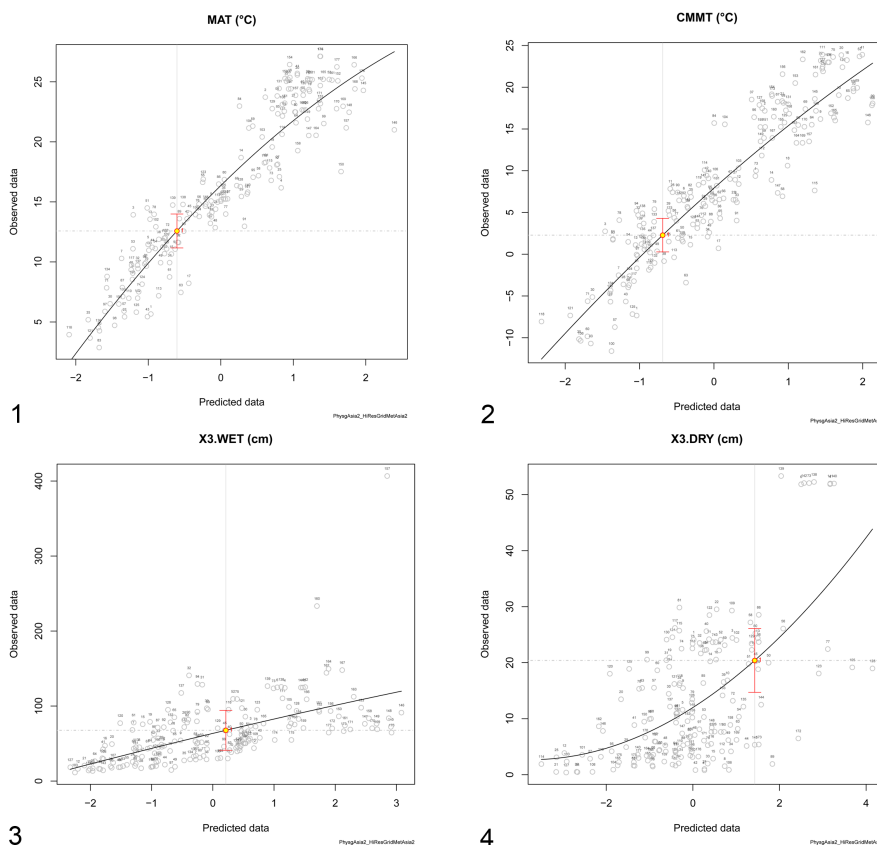
Figure 6. CLAMP climate inference for the macrofossil assemblage of Eskihisar (same level

as PZ 2). **1.** Mean annual temperature (MAT). **2.** Coldest month mean temperature (CMMT).

3. Precipitation of the three wettest months. **4.** Precipitation of the three driest months.

633

Table 1

Latest occurrence W Eurasia	Fossil-taxon (genus level)	wEUR[f]	EA	eNA	wNA	SA	AF	AUS
	Ephedra	+	+	+	+	+	+	
Pliocene?[a]	Glyptostrobus		+					
Taxodium-type, < 0.1 Ma[a]	Taxodium			+	+			
0.5-0.4 Ma[a]	Cathaya		+					
	Cedrus	+	+					
	Picea	+	+	+	+			
	Pinus	+	+	+	+			
0.4-0.3 Ma[a]	Tsuga		+	+	+			
	Acer	+	+	+	+			
late Pliocene[b]	Ailanthus		+					
	Alnus	+	+	+	+	+		
no data	Apios		+	+				
	Betula	+	+	+	+			
	Buxus	+	+	+	+	+	+	
	Buxus (balearica type)	+	+					
	Carpinus	+	+	+				
< 0.1 Ma[a]	Carya		+	+				
	Castanea	+	+	+				
Pliocene[c]	Cedrelospermum†	+	+		+			
	Celtis	+	+	+	+	+	+	+
	Centranthus	+	+					
	Corylus	+	+	+	+			
Pleistocene[d]	Decodon			+				
	Drosera	+	+	+	+	+	+	+
	Erica	+					+	
	Erodium	+	+	+	+	+	+	+
0.6 Ma[a]	Eucommia		+					
	Euphorbia	+	+	+	+	+	+	+
	Fagus	+	+	+				
	Fraxinus	+	+	+	+			
	Ilex	+	+	+	+	+	+	+
	Juglans	+	+	+	+	+		
	Linum	+	+	+	+	+	+	+
	Liquidambar	+	+	+				
	Lonicera	+	+	+	+			
	Ludwigia	+	+	+	+	+	+	+
Pliocene[d]	Mahonia		+					
	Nitraria	+	+				+	+
	Ostrya	+	+	+				
	Parrotia	+						
	Persicaria	+	+	+	+	+		
	Phragmites	+	+	+	+	+	+	+
no data	Picrasma		+	+	+	+		
Pleistocene[e]	Podocarpium †	+	+					
	Polygonum	+	+	+	+			
	Populus	+	+	+	+			
	Pterocarya	+	+					
	Quercus	+	+	+	+	+		
	Rumex	+	+	+	+	+		+
	Salix	+	+	+	+	+		
	Scabiosa	+					+	
	Smilax	+	+	+	+	+	+	+
14.8-13.8 Ma	Smilax (havanensis group)			+		+		
	Sorbus	+	+	+	+			
	Sparganiium	+	+	+	+			+
	Tilia	+	+	+	+			
	Typha	+	+	+	+	+	+	+
	Ulmus	+	+	+	+			
	Viburnum	+	+	+	+	+		
	Zelkova	+	+					
	No. of genera/region	48	54	44	36	21	16	13
		wEUR[f]	EA	eNA	wNA	SA	AF	AUS

Table 1. Genus-level biogeographic affinities of fossil-taxa of the Yatağan Basin floras.

[a]Magri et al., 2017; [b]Corbett & Manchester, 2004; [c]Jia et al., 2015; [d]Martinetto, 2001; [e]Wang et al., 2007; [f]including northern Africa; † extinct genus.

638   wEUR = western Eurasia, EA = East Asia, eNA = eastern North America, wNA = western

639   North America, SA = South America, AF = Africa (excluding northern Africa), AUS =

640   Australia.

641

Table 2

Pollen Zone	AP	NAP	
Hüssamlar	90	10	16.8 Ma
Kultak	90	10	MN5
Karacaağaç	96	4	
Tınaz PZ1	75,00	25,00	14.8 Ma
	94,20	5,80	MN6
	0,00	0,00	
	0,00	0,00	
	75,58	24,42	
	85,00	15,00	
	0,00	0,00	
Tınaz PZ2	54,13	45,87	
	89,22	10,78	
	62,04	37,96	
	86,82	13,18	
	28,66	71,34	
	46,04	53,96	
	0,00	0,00	13.9 Ma
Tınaz PZ2-3	19,01	80,99	(?)MN7+8 *
	0,00	0,00	MN7+8
	50,44	49,56	
Yenieskihisar	67,00	33,00	13.2 Ma

* = perhaps linked with 13.9-13.8 Ma cooling event
(Holbourn et al., 2014)
AP = arboreal pollen (angiosperms)
NAP = non-arboreal pollen (angiosperms)
wavy line = profiles separated by tens of meters
of sediment barren of pollen

642

643 **Table 2**. Arboreal to non-arboreal pollen ratios in southwestern Anatolia across the MCO,

644 MMCT and subsequent cooling phase.